JOURNAL OF GEOMAGNETISM AND GEOELECTRICITY VOL. 22, NO. 1-2, 1970

An Introduction to Induction Anomalies

Ulrich SCHMUCKER

Institut fuer Geophysik, Universitaet Goettingen

(Received January 12, 1970)

Abstract

The inductive response of the electrically conducting Earth's interior to geomagnetic variations can be inferred from the magnetic *Z-H* or the magneto-telluric *E-H* relations. In the absence of lateral non-uniformities of the electrical resistivity within a distance range which is comparable to the depth of penetration these relations are expressible by a single transfer function in in the frequency-wave number domain or by convolutions in the frequency-space domain. Lateral non-uniformities within the mentioned range produce anomalous *Z-H* and *E-H* relations. The resulting induction anomaly is dependent on the direction of source-field polarization with respect to subterranean resistivity gradients. The interpretation proceeds from a known or assumed normal inductive response for a layered Earth which is defined on a regional scale and serves as normal reference for lateral non-uniformities to be investigated. The uniform internal part of D_{st}-variations shows that the mantle resistivity below 600 km depth is of spherical symmetry. The internal part of *Sq*-variations appears to be affected by lateral non-uniformities in the upper 400 km. For fast variations (e.g. bays) the inductive shielding by oceans and interspersed sedimentary basins on land becomes significant. In addition to this surface effect there exist regional and local variation in the depth of penetration of fast variations which originate from non-uniformities in the uppermost mantle.

Transient magnetic fields pass through electrically conducting matter with amplitude reduction and phase rotation. We are concerned here with the inductive skin-effect of natural geomagnetic variations which they undergo within the Earth's interior. These variations are very slowly oscillating and can be regarded as quasi-stationary on a global scale. The pertinent resistivity (ρ)-frequency (f) parameter is the *skin-depth value*

$$p=\frac{1}{2\pi}\sqrt{\frac{\rho}{\mu f}}, \qquad (1)$$

a characteristic length for material of the magnetic permeability μ (emu-cgs units). If the frequency is measured in cycles per hour (cph) and the resistivity in Ωm, we obtain $p=30.2\sqrt{\rho/f}$(km) with $\mu=1$ as free-space permeability in electromagnetic units.

Geomagnetic induction studies involve frequencies from a few cycles per minute to fractions of a cycle per day. This yields in combination with internal resistivities between 1 and 10^4 Ωm skin-depth values in the kilometer range. The depth z^* at which the main inductive attenuation of geomagnetic variations occurs can be inferred from Table 1.

The inductive response of the Earth's interior to the spectrum of geomagnetic varia-

tions and thereby the internal resistivity distribution can be studied by two complementary methods: We can observe (i) the vertical magnetic component Z (*magnetic method*) or (ii) the tangential electrical component E (*magneto-telluric method*) of a transient surface field, setting either one of them in relation to the horizontal magnetic component H within a certain distance range around the point of observation.

This introduction reviews the theory and general results of geomagnetic induction studies without particular reference to their geophysical significance. Other contributions to this volume will show that the electrical resistivity is an important parameter for the state of internal matter, in particular its thermal state. Inhomogeneities in ρ have been correlated successfully with those of other physical properties, thus giving new insight into an upper mantle of considerable lateral complexity.

1. Inductive response in the absence of lateral non-uniformities

Suppose the resistivity beneath a plane Earth's surface is only a function of depth, $\rho(z)$, within a distance range to be defined later; z is vertically down and the Earth's surface forms the (x, y)-plane of right handed coordinates (x, y, z). A transient electromagnetic field of external origin induces currents in the conducting matter beneath the surface.

Table 1: Inductive scale-length $C_m{}^n(\omega)$ and $C(\omega, 0)$ for the attenuation of geomagnetic variations within the Earth (Eq. 7 and 24).

Variation-type	Period (hours)	n	m	$S_n{}^{m1)}$	z^* (km)	$\frac{1}{2}p^{*2)}$ (km)	ρ^* (Ωm)	ρ_a (Ωm)	ρ_s (Ωm)
D_{st}	(72)	1	0	.35 (.36)	710				
1. Sq-harmonic	24	2	1	0.35+i·0.09	740	275	14	58	
				(.41 .08	575	225	9	35	10)
2. Sq-harmonic	12	3	2	.43 .14	450	250	23	49	
				(.43 .12	465	210	16	47	10)
3. Sq-harmonic	8	4	3	.38 .15	460	220	26	71	
				(.42 .14	400	200	22	55	10)
Bays, ocean	1				4.2	27	3.1	1.6	0.25
Bays, continent	1				72	113	57	40	2
Bays, continent	1				167	121	65	94	10
Bays, continent	1				203	103	47	114	10^4
Fluctuations, ocean	0.1				1.4	3	.39	.25	0.25
Fluctuations, continent	0.1				4.7	21	20	10	2
Fluctuations, continent	0.1				41	62	169	122	10
Fluctuations, continent	0.1				121	45	88	368	10^4

1.) From *Chapman's* analysis (*Chapman and Bartels*, 1940 chap. 20.7 and 20.11); in parenthesis: theoretical values for model d^*, Fig. 4, and continental cover ($\rho_s=10\Omega$m).

2.) D_{st} and Sq: calculated from $S_n{}^m$ according to *Eq.* 23; Bays and fluctuctuations: calculated for model d^*, Fig. 4, and a top layer of the resistivity ρ_s (last column), 4 km thick; source field regarded as quasi-uniform (k=0).

The surface field of these currents when set in relation to the inducing source field characterizes the inductive response of the lower half-space.

This response can be expressed in terms of a single transfer function $C(\omega, k)$ when we represent the transient surface field, given for $z=0$ as function of time t and position $\boldsymbol{r}$, by a two-dimensional spectrum with exp $(i\,[\omega\, t+\boldsymbol{k}\cdot\boldsymbol{r}])$ as common time-distance factor for each spectral component of Z, E, and H (s. above); $\omega=2\pi f$, and $\boldsymbol{r}$ denotes the radius vector from some point of origin. The wave-number vector $\boldsymbol{k}$ describes a quasi-stationary spatial modulation. It is *not* the wave number of a true electromagnetic wave, propagating with the speed of light. An extension of this spectral representation to spherical harmonics can be found in the Appendix.

For simplicity we regard now the source field as two-dimensional and consider the field components E, H, and Z in x, y, z-direction as functions of t and x, e.g. $H(t, x)$. The first transformation into the frequency-space domain gives

$$\tilde{H}(\omega, x)=\int_{-\infty}^{+\infty} H(t, x)\, e^{-i\omega t}dt \qquad (2)$$

and the second into the frequency-wave number domain

$$\hat{H}(\omega, k)=\int_{-\infty}^{+\infty} \tilde{H}(\omega,x)e^{-ikx}\, dx \qquad (3)$$

as complex-valued Fourier transforms. The transfer function which describes the inductive response of the conducting lower half-space in the (ω,k)-domain can be introduced in the symmetrical form (cf. for instance Schmucker, 1970)

$$\begin{aligned}\hat{Z}(\omega, k)&=ikC(\omega, k)\cdot\hat{H}(\omega, k)\\ \hat{E}(\omega, k)&=i\omega\mu C(\omega, k)\cdot\hat{H}(\omega, k).\end{aligned} \qquad (4)$$

$C(\omega, k)$ is a length and its real part a direct indicator for the depth at which the main attenuation of the observed surface field occurs. For a uniform substratum with the skin-depth value $p(\omega)$

$$C(\omega, k)=\left[\left(\frac{1+i}{p(\omega)}\right)^2+k^2\right]^{-1/2}. \qquad (5)$$

When the analysis proceeds from a separation of the transient magnetic surface field into parts of external and internal origin (*Schuster's* method), the resulting ratio of internal to external part for each spectral component is

$$S(\omega, k)=\frac{1-kC(\omega, k)}{1+kC(\omega, k)}. \qquad (6)$$

The inductive scale-length $C(\omega, k)$ can be derived obviously either from magnetic observations alone or from combined magnetic and electric (telluric) observations. We observe that the magnetic $\hat{Z}/\hat{H}$-ratio gives this generalized skin-depth C in relation to the wave length $L=2\pi/k$ of the inducing source field mode. Z-variations disappear altogether when $L\gg|C(\omega, k)|$. It implies that the Z-component of the external source field is compens-

ated for $z=0$ by the opposite Z-component of the field which the induced currents in the lower half-space produce at the surface. The internal attenuation of the source field is then purely inductive as it applies to fast geomagnetic variations in mid-latitudes (Sect.5). The transfer function C approaches under these conditions a finite limiting value

$$C(\omega, 0)=\frac{z^{*}(\omega)}{Z^{*}(\omega)}-\frac{i}{2}p^{*}(\omega)=\sqrt{\frac{1}{2}p_a(\omega)}e^{-i\varphi(\omega)} \qquad (7)$$

which is fundamental for the magneto-telluric method of *Tikhonov and Cagniard* (s. below). When to the contrary L is small in comparison to the ambient skin-depth values, the internal attenuation of the source field by induction is negligible and $C(\omega,k)$ approaches k^{-1}.

There are several convenient numerical techniques to calculate $C(\omega,k)$ for any given resistivity model (*Tikhonov and Lipskaya*, 1952; *Wait*, 1953; *Cagniard*, 1953). The inverse problem to infer $\rho(z)$ from a given response function $C(\omega,k)$ appears to be basically a single solution problem. In praxis difficulties arise from two sources: (i) The inductive response, undisturbed by lateral non-uniformities, usually is known only for a very limited part of the frequency spectrum (cf. Sect. 5); (ii) the inductive response is always a very smooth function of frequency, even when the resistivity to be inferred is a discontniuous and rugged function of depth. Furthermore, high resistivities at greater depth are effectively concealed by overlying material of low resistivity (Fig. 1).

The evaluation of magnetic or magneto-telluric observations in the (ω, k)-domain requires two consecutive Fourier transformations. The second one from the space into the wave number domain (Eq. 3) is impracticable when the observations have not been carried out over the full width of the inducing source field or when there exist large-scale lateral non-uniformities. In both cases we are forced to derive the inductive response from observations within a limited range of x which can be done in two ways:

(i) The source field is approximated for each freqency component by a single spatial harmonic, $\exp(ik_0 x)$. Eq.4 is then evaluated with the appropiate time harmonics at a single site, yielding a local estimate of the inductive response for $k=k_0$. We may also eliminate any source-field-dependence by setting k_0 formally to zero in the case of a purely inductive attenuation (s. above) and obtain the *Tikhonov-Cagniard* approximation

$$\tilde{Z}(\omega, x)=0 \qquad (8)$$
$$\tilde{E}(\omega, x)=i\omega\mu C(\omega, 0)\cdot\tilde{H}(\omega, x)\,.$$

The implications of the resultining transfer function $C(\omega,0)$ for the internal resistivity distribution can be made more transparent by converting it into an apparent resistivity versus frequency or depth function, based on the value for a uniform substratum. *Tikhonov and Cagniard* derive an apparent resistivity $\rho_a(\omega)$ from the modulus of $C(\omega, 0)$ by defining $p_a(\omega)$ in Eq. 7 as skin-depth value for ρ_a (cf. Eq. 1). The change of ρ_a with decreasing frequency resembles in a smoothed form the change of the true resistivity with depth and the inversion consists basically in the adoption of a fitting depth scale.

When the amplitude and phase of $C(\omega, 0)$ are considered separately (even though they

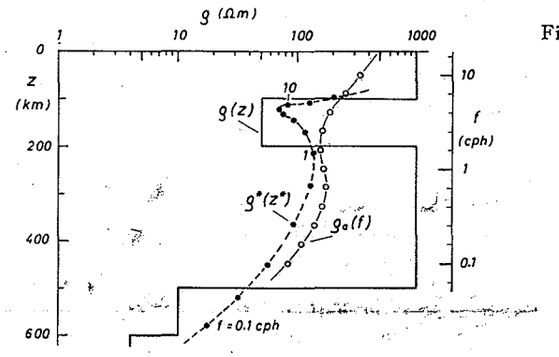

Fig. 1. Resistivity model $\rho(z)$ and its inductive response to a quasi-uniform field, given by the *Tikhonov-Cagniard* apparent resistivity $\rho_a(f)$ as function of frequency f (right scale) and by the modified apparent resistivity $\rho^*(z^*)$ as function of depth z^* with f as curve parameter. Notice the "shielding effect" of the low-resistivity layer between 100 and 200 km depth upon the underlying high-resistance zone between 200 and 500 km.

are as functions of frequency not truly independent), we obtain a first-order approximation of the desired resistivity distribution by regarding $p^*(\omega)$ in Eq. 7 as skin-depth value for the modified apparent resistivity ρ^* at the depth z^* (*Schmucker*, 1970). If the argument of $C(\omega,0)$ lies between $-45°$ and $-90°$ ρ^* is the resistivity of a substitute uniform conductor at the depth $\left(z^*-\frac{1}{2}p^*\right)$ for the considered frequency. Both interpretations of the inductive scale-length for a quasi-uniform source field are shown in Fig. 1.

(ii) The unrestricted representation of the inductive response for all wave numbers in the (ω,x)-domain leads to convolution integrals, relating the time harmonics of E and Z to those of H within a certain distance range around the point of observation. For convenience we use as convolution kernels the transforms of $C(\omega, k)$ and $ikC(\omega, k)$ into the (ω, x)-domain, denote them with N and M, and obtain according to the convolution theorem of Fourier products from *Eq.* 4

$$\tilde{Z}(\omega, x)=M(\omega, x) * \tilde{H}(\omega, x)$$
$$\tilde{E}(\omega, x)=i\omega\mu[N(\omega, x) * \tilde{H}(\omega, x)]. \qquad (9)$$

The implied operation on M and H, for instance, is

$$\int_{-U}^{+U} M(\omega, u)\cdot\tilde{H}(\omega, x-u)du$$

with $U\to\infty$. Because $C(\omega,k)$ is an even function of k, N and M are one-sided cosine and sine transforms, viz.

$$M(\omega, u)=-\frac{1}{\pi}\int_0^\infty kC(\omega, k)\sin(ku)dk$$
$$N(\omega, u)=\frac{1}{\pi}\int_0^\infty C(\omega, k)\cos(ku)dk \qquad (10)$$

with singular point at u=0 (Fig. 2). Both kernels go exponentially to zero, when the distance u exceeds the real and imaginary part of $C(\omega, 0)$. It is therefore sufficient to extend the convolution integrals in Eq. 9 over a distance range $\pm U$ where U is equal to or a bit larger than z^* and $\frac{1}{2}p^*$, respectively.

This leads to the important conclusion that $C(\omega, 0)$ is not only a vertical, but also a lateral scale-length, indicating depth and width of the cross-section which effectively determines the inductive response at the point of observation.

The inverse of the second transformation in Eq. 10 yields for $k=0$

$$C(\omega, 0)=\int_{-\infty}^{+\infty} N(\omega, u)du \qquad (11)$$

When $\tilde{H}(\omega, x)$ is sufficiently uniform within the range of the kernels M and N, given by $C(\omega, 0)$, we may consider it in the convolution integrals of Eq. 9 as a constant and obtain in virtue of Eq. 11 again the *Tikhonov-Cagniard* approximation. For a general distribution $\rho(z)$ the kernels M and N have to be determined by a numerical integration over the pertinent transfer function $C(\omega,k)$ according to Eq. 10. Two analytical solutions may be illustrative. The kernels for a uniform substratum with the skin-depths value $p(\omega)$ follow from Eq. 5 as

$$M(\omega, u)=-\frac{1+i}{\pi p(\omega)}K_1\left(\frac{1+i}{p(\omega)}u\right)$$
$$N(\omega, u)=\frac{1}{\pi}K_0\left(\frac{1+i}{p(\omega)}|u|\right) \qquad (12)$$

where K_0 and K_1 denote modified Bessel functions of the second kind. A perfect conductor beneath a non-conducting layer of the thickness h^* has the kernels

$$M(\omega, u)=-\left\{2h^*\sin h\left(\frac{\pi u}{2h^*}\right)\right\}^{-1}$$
$$N(\omega, u)=\frac{1}{\pi}ln\left\{ctnh\left(\frac{\pi|u|}{4h^*}\right)\right\} \qquad (13)$$

because the pertinent transfer function is $C(\omega, k)=k^{-1}tanh(kh^*)$. These kernels are shown in Fig. 2.

2. Inductive response in the presence of lateral non-uniformities

The two-fold implication which has been derived in the preceeding section for the inductive scale-length $C(\omega, 0)$ of a quasi-uniform source field allows the following distinction between a normal and anomalous state: If $\rho=\rho(z)$ is solely a function of depth z within the depth-distance range $|C(\omega, 0)|$ around the point of observation, the inductive response at that point is termed *normal*, otherwise *anomalous*. Henceforth, all quantities referring to the normal state carry the subscript "n" and those referring to the anomalous state the subscript "a", assuming that the latter is superimposed as a local perturbation upon the normal state ($Z=Z_n+Z_a$,....., $\rho=\rho_n+\rho_a$).

In the *normal state* the methods of Sect. 1 can be applied to infer a resistivity-depth profile $\rho_n(z)$ for the above mentioned depth-distance range. In the *anomalous state* the Z–H or E–H relations when freed from their normal component reflect local deviations from a layered distribution ρ_n, thus relating the *induction anomaly* in the magnetic and electric variation field to a subterranean *resistivity anomaly* ρ_a. This anomalous state is highly

frequency dependent. The inductive response at some site may be normal at high frequencies but anonalous at low frequencies when the inductive scale-length $C(\omega, 0)$ becomes in its real or imaginary part comparable to the scale-length L_a of lateral non-uniformities. The induction anomaly disappears again, at least in Z and H, at very low frequencies when $C(\omega, 0)$ in its real and imaginary part is much larger than L_a (s. below).

There are two types of induction anomalies, namely those which are situated within an extended region of normal response (Fig. 3) and those which occur at the border of two different normal regions (Fig. 2). Either one of these regions may be closer to what may be regarded as global norm, even though such a norm is presently ill defined and presumably a distinction has to be made between oceans and continents (cf. Sect.3).

The anomalous and normal state differ in two important aspects: (i) The normal variation field originates to nearly equal parts from external and internal sources. Induction anomalies, however, are of purely internal origin which implies that Z_a and H_a as functions of location are interdependent. This can be used to test the consistency of observed Z and H-anomalies. (ii) Normal Z–H or E–H relations are the same for all directions of a polarized source field (for a given wave number or wave number spectrum). The anomalous inductive response, in contrast, is critically determined by any source field polarization in relation to subsurface lateral resistivity gradients. We distinguish here two special cases:

Consider a two-dimensional resistivity distribution $\rho(x, z)$ in right handed rectangular coordinates (x,y,z) which is exposed to a two-dimensional source field (Fig.2). *E-polarization* (in y-direction) implies that the transient magnetic vector is confined to the (x, z)-plane. The induced currents which are [illegible] in y-direction are drawn together where low resistivities come closer to the surface than elesewhere, and vice versa. This "*lateral skin-effect*" produces in Fig. 2, a magnetic Z-anomaly at station "2", while E increases on the same profile smoothly from its low normal value at "1" to its high normal value at "3".

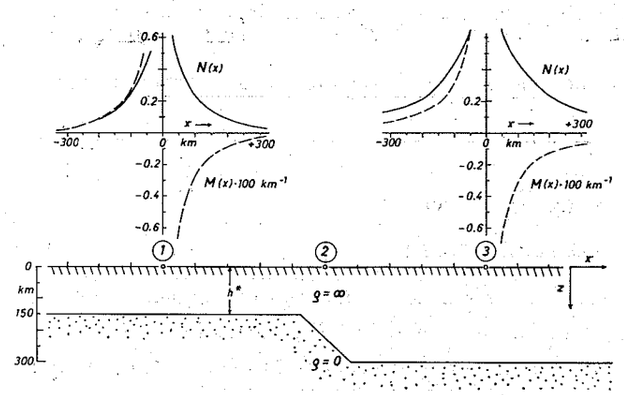

Fig. 2. Two-dimensional resistivity model $\rho(x, z)$. The slope in the surface of the perfect conductor causes an induction anomaly of transient ~~geomanetic and~~ geomagnetic and geoelectric variations at "2", depending on the direction of source-field-polarization (cf. text). The inductive response at "1" and "3" is different, but normal because the convolution kernels M and N (*Eq.* 13) for the Z-H and E-H relations at those stations, shown above the profile, do not extent into the anomalous zone near "2". The reduced depth of the perfect conductor causes a small E/H-ratio at "1" in comparison to that at "3". The same applies to Z/H for a given source-field gradient.

In the case of *H-polarization* (in y-direction) the situation is reversed. The induced

currents, now confined to the (x,z)–plane, are deflected up and down in response to lateral changes in ρ. These deflections perturb the superficial E-field, but have almost no influence upon Z and H. In Fig. 2 E is sharply reduced near station "2" above the slope in the surface of the perfect conductor when going from station "3" to "1". The transition from the high normal Z at "3" to the low normal Z at "1" is in contrast gradual. In the case of a quasi-uniform source field Z_n is zero and no magnetic induction anomaly is observed (Eq. 8).

This directional dependence makes it necessary to consider the anomalous inductive response separately for the two orthogonal horizontal directions of source field polarization, i. e. the Z-H and E-H relations above resistivity anomalies have matrix form. This matrix of transfer functions is usually formulated and derived in the frequency-space domain under the specific assumption that the normal response is that or nearly that of a quasi-uniform source field.

The depth distribution of the induced currents is then, for a given normal distribution $\rho_n(z)$, a function of frequency only. Lateral non-uniformities produce either a re-arrangement of these normal currents (E-polarization), their deflection (H-polarization), or a combination of both effects. Their strength depends linearly on H_n and the same applies therefore to the surface induction anomaly in Z, H, and E (cf. also *Fanselau and Treumann*, 1966).

Let H and D, respectively E_N and E_E, denote the orthogonal components of the transient magnetic and electric vector in the horizontal plane, e. g. their north and east components.

The linear dependence of their anomalous parts on H_n and D_n allows then the formulation

$$\tilde{Z}=a\tilde{H}+b\tilde{D} \qquad (14)$$

$$\tilde{E}_N=i\omega\mu(c_{NH}\tilde{H}+c_{ND}\tilde{D})$$

$$\tilde{E}_E=-i\omega\mu(c_{EH}\tilde{H}+c_{ED}\tilde{D}).$$

The complex-valued transfers a, b, c_{NH},...describe as functions of frequency and location the induction anomaly in a normalized form for H and D polarization at the point of observation (s. below). At a "normal" site Z would be unrelated to H and D in the statistical average over all directions of polarization, yielding $a=b=0$. In the electrical matrix only the cross-terms c_{NH} and c_{ED} would disappear, while c_{ND} and c_{EH} both become equal to $C(\omega, 0)$ in accordance with Eq. 8.

In view of the subsequent interpretation it is of advantage to relate induction anomalies to the normal variation field as it may have been observed at some distance from the anomaly.—If the anomaly lies at the border of two normal regions, one of them is chosen to represent the normal state. The anomalous state when added to it has to merge properly into the normal state of the second region. This condition can be used to test theoretical model calculations (cf. *Schmucker*, 1970; Sect. 7.3).—Hence, in place of Eq. 14 we write

$$\tilde{Z}=z_H\tilde{H}_n+z_D\tilde{D}_n \qquad (15)$$

and obtain now in z_H and z_D the transfer functions for the normalized anomalous response for north and east polarization of the source field. The transfers a and b are readily expressed in terms of z_H, z_D, and the four other transfer functions connecting the anomalous parts in H and D to H_n and D_n. The induction anomaly in E can be normalized in the same way.

Parkinson (1959) *and Wiese* (1962) introduced a now widely used vector presentation of the transfer functions a and b or z_H and z_D (cf. *Edward' and Untiedt's* contribution to this volume). These induction arrows delineate, when displayed on maps for an array of observation points, the location and trend of subsurface resistivity anomalies. A description of statistical methods to determine the transfer functions from actual observations can be found elsewhere (*Everett* and *Hyndman*, 1967; *Schmucker*, 1970).

There now remains the task of inferring the depth and size of resistivity anomalies from surface observations with as little ambiguity as possible. This requires (i) that a normal reference distribution $\rho_n(z)$ is available and (ii) that the induction anomaly has been analysed for various frequencies so that the frequency of maximum anomalous response is known (s. below).

Up to now the interpretation of induction anomalies has been based on two types of models, namely on non-unifom thin sheets or shells and on two-dimensional resistivity distributions beneath a plane Earth's surface. The assumption of a thin sheet implies that, for sufficiently slow variations, E and Z may be regarded a uniform over the thickness d of the sheet or shell which is bounded by non-conducting material. The non-uniformity is contained in a variable total or integrated conductivity

$$\tau=\int_o^d \frac{dz}{\rho(z)} \qquad (16)$$

(*Price*, 1949). This method has been applied to induction anomalies of shallow origin, notably to those near coast lines or sedimentary basins (cf. *Rikitake*'s monograph, 1966; also *Rikitake*, 1967, 1968). Such surface anomalies are coupled by mutual induction to the deep resistivity structure, provided that their lateral width is comparable to the inductive scalelength $C(\omega, 0)$ for the underlying (normal) resistivity distribution $\rho_n(z)$.

In the case of a two-dimensional resistivity structure the transfer functions for the anomalous parts in E, Z, and H have their simplest form when they refer to pure E- or H-polarization of the source field. This requires that empirical transfer functions which are to be interpreted by a two-dimensional model are transferred first to a direction normal and parallel to the trend of the anomaly which can be inferred from the anomalous behaviour in Z. The induction problem to be solved is a *disturbed skin-effect problem* when H_n is assumed to be quasi-uniform and $Z_n=0$. Solutions have been obtained mainly with numerical methods, using iteration or matrix inversion techniques (cf. *Madden and Swift*, 1969;. *Wright*, 1969). Approximation methods for the treatment of the two-dimensional disturbed skin-effect problem have been developed by *Fanselau and Treumann* (1966) and by *Scheube* (1966).

In two limiting cases the induction problem can be reduced to a quasi-static one.

(i) Suppose the scale-length of a resistivitity anomaly is small in comparison to the skindepth values within and around the anomaly. We may then neglect the anomalous part in E due to locally disturbed self-induction, leaving $E_n(z)$ as driving force of the induced currents. When $j_n(z)=E_n(z)/\rho_n(z)$ denotes the (known) normal current density at some distance from the anomaly, its super-imposed anomalous component within the resistivity anomaly is

$$j_a=(-\rho_a/\rho)\cdot j_n \qquad (17)$$

(*Ohm's* law). An integration according to the formula of *Biot-Savart* yields the induction anomaly in Z and H at the Earth's surface.

(ii) The in-phase part of the normal inductive response can be explained by a perfect substitute conductor at the frequency-dependent depth $z^*(\omega)$ at which the main attenuation by induction currents occurs (Eq. 7). Lateral resistivity variations at this depth have approximately the effect of an undulatory interface between non-conducting and perfectly conducting matter. This implies that the transfer functions of the induction anomaly z_H, z_D,...are real. For a given shape of the interface they can be found by satisfying the static boundary condition that the transient magnetic vector is tangential to and the transient electric vector zero on the interface. The shape can be inferred also directly from the transfer functions by constructing the internal pattern of field lines beneath the induction anomaly. This requires a downward extension of the surface field. Each field line represent one possible interface between non-conducting and perfectly conducting matter and the choice is made according to the normal depth $z^*(\omega)$ at the considered frequency (*Schmucker*, 1959 and 1970).

Both methods have been used to calculate the induction anomaly in H (E—polarization) above a bulge of low resistivity, extending into a high-resistivity top layer (Fig. 3). For sufficiently high frequencies the attenuation is strong, even in the top layer, and the resistivity anomaly is not reached by the variation field at all. At about 5 cph the attenuation in the top layer is weak and the skin-depth value of the substratum is small in comparison to the diameter of the bulge, implying that the variation field hardly penetrates into the interior of the bulge. The induction anomaly is now at its maximum and nearly in-phase as if the substratum with the inclusion of the bulge were perfectly conducting.

A further reduction of the frequencies means that the main attenuation takes place well beneath the level of the bulge and that we may use *Ohm's* law to find the current distribution within the bulge (Eq. 17). The resulting induction anomaly is small and shows a distinct out-of-phase component. Ultimately, at very low frequencies, the magnetic and electric induction anomaly for E-polarization disappears altogether because the relative strength of currents which are induced in the depth range of the bulge becomes negligible. The induction anomaly in E for H-polarization, on the other hand, approaches a finite limiting value when, at very low frequencies, the distortion of the electric field in the neighborhood of the bulge becomes that of a quasi-static field.

In summary, the anomalous inductive response goes through a maximum at that frequency at which the normal variation field has its main attenuation in the depth range

of the resistivity anomaly. This depth can be determined therefore with some confidence, providing that reliable estimates of the normal distribution $\rho_n(z)$ are available in the considered area. If there exist at some intermediate depth lenses of low resistivity within a high-resistivity environment, they must have a conducting connection to the depth range of main attenuation in order to produce a detectable induction anomaly at the surface.

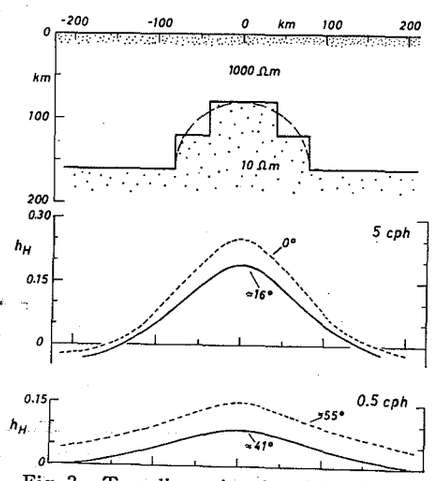

Fig. 3. Two-dimensional uplift of low resistivities (10 Ωm) into a high-resistivity top layer. The induction anomaly in H (horizontal magnetic component) for E-polarization is shown for two frequencies, 5 and 0.5 cycles per hour. The curves give the modulus of the transfer function $h_H=H_a/H_n$. They have been derived with approximation methods (dashed, ct. text) and with a matrix inversion technique (solid, courtesy of Dr. *J.A. Wright*), the latter yielding the "correct" solution of the disturbed skin-effect problem. The approximate phase lead of H_a with respect to H_n is indicated. The central maxima of h_H reflect the current concentrations in the uplift. They disappear toward very low and very high frequencies (cf. text).

3. Basic resistivity models for the Earth's interior

Induction anomalies of geomagnetic variations may be compared to travel-time anomalies of seismic P and S waves. We have in either case local or regional deviations from a global norm which in seismology is known with great precision in form of the *Jeffreys-Bullen* traveltime curves. Their geomagnetic equivalents are the inductive response functions $C(\omega, k)$ or $C_n^m(\omega)$ which for convenience may be expressed as apparent resistivity versus frequency or depth curves (Table 1). Our present knowledge about ocean basins is quite limited in this respect and the following statements apply to the continental substructure.

The inductive attenuation of very slow variations with periods of eight hours or longer occurs deep within the upper mantle. This has been clearly established by a global analysis of their magnetic Z-H relations. The modified apparent resistivities ρ^* for Sq-variations in Table 1 indicate that we may expect a resistivity of roughly 25 Ωm at 400 km depth with the tendency to decrease with increasing depth. Because these slow variations penetrate through the uppermost mantle with little attenuation they cannot yield more than a lower permissible limit for the resistance above 400km. Such a limit is *Price and Lahiri's* (1963) model "*d*" which suggests an exponential decrease according to $\rho(z)\sim 250\cdot\exp(-0.058\,z)$ Ωm where z denotes the depth in (km). Their alternative model "*e*" shows that the upper mantle can be regarded also as effectively non-conducting down to a considerable depth when we add a highly conductive surface layer and assume a sharp resistivity reduction to 1 Ωm or less at 600km (Fig. 4). Both models are equivalent as far as their inductive response to slow D_{st} and Sq-variations

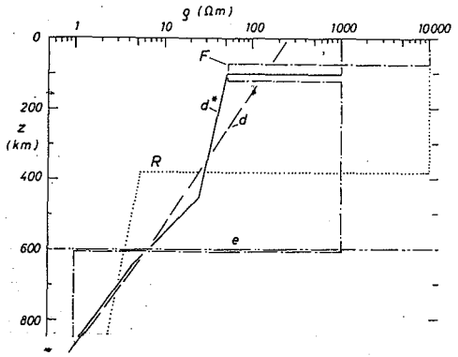

Fig. 4. Resistivity models for the upper mantle beneath continents. Model "*d*" and "*e*" (*Lahiri and Price*, 1939) represent limiting distributions with regard to the magnetic internal part of D_{st} and *Sq*-variations. Both models include a thin top layer (not shown) with integrated conductivities of 2000 Ω^{-1}(d) and 5100 Ω^{-1} (e). Model "*R*" (*Rikitake*, 1950) is in particular good agreement with the internal part of D_{st} and ultra-long periodicities in geomagnetic activity. Model "*d**" and "*F*" (*Fournier et al.*, 1963) are modified versions of model "*d*" and "*e*." They include within the uppermost mantle (80-100 km) a zone of low resistivity in accordance with magneto-telluric sounding curves (Fig. 6).

is concerned (Fig. 5).

It has not been possible yet to narrow this wide range of possible distributions by evaluating the *Z-H* relations of faster and therefore less deeply penetrating variations, utilizing for instance bay events (Sect. 5). The best information available about the upper 100 to 200 km comes from magneto-telluric soundings in areas without a well conducting cover of unfolded young sediments. Very fast fluctuations with periods in the minute and second range yield in such areas very high apparent resistivities ρ_a between 10^3 and 10^4 Ωm, verifying that the crust and uppermost mantle are indeed very poor conductors as in model "e" (Fig. 6). The usually distinct decrease of ρ_a with increasing period implies that the true resistivity is reduced to about 50 Ωm at 80 km depth, even though this depth appears to be subject to large regional variations (cf. *Caner's* contribution to this volume). It is undecided whether such low values are confined to an mantle "low resistivitity layer" within a model "e" type distribution as prodosed by *Fournier et al.* (1962), *Porstendorfer* (1965) and others or whether they merge smoothly into model "*d*" (cf. also *Rikitake*, 1962). The required modifications in the upper portion of model "d" would have to be such that the inductive response to D_{st} and *Sq*-variations remains unchanged as it is more or les the case for the here proposed model *d** in Fig. 4. *Fournier*-type models need some amendments in this respect because they yield an internal *Sq* which is too small (Fig. 5).

Model *d** which is similar to *Cantwell's* model (1960) includes two zones of rapidly changing resistivity. A first reduction from 1000 Ωm to 50 Ωm near 100 km depth appears to be mainly temperatuare controlled. The second reduction from 25 Ωm to 5 Ωm between 400 and 600 km may reflect the phase transition from olivine to spinel and the increase of the iron content of these minerals which presumably takes places in mantle region *C* of *Bullen's* classification. In the intermediate depth range detween 100 and 400 km the temperature effect upon ρ could be largely balanced by the opposing effect of increasing pressure, assuming that the ambient temperature gradient is small, i. e. in the order of 1°C/km (*Hughes*, 1955).

Henceforth, model *d** serves as (continental) norm. For the calculations of the attenuation curves in Fig. 7, 9, and 11 it is approximated by a 13-layer model, each layer being

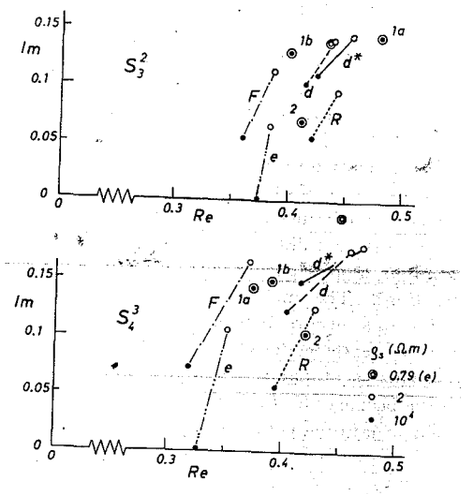

Fig. 5. Observed and theoretical rations S_n^m of internal to external part of *Sq*-variations, shown in the complex plane for the 2nd and 3rd time harmonic. Large dots: Empirical ratios for the global *Sq*-field during the equinoxes of 1902 (1*a*), 1905 (1*b*), and 1933 (2), derived by *Chapman* (cf. *Chapman and Bartels*, 1940; chap. 20. 4; 1*a* and 1*b*) and by *Hasegawa* (1936, 2). Small dots and open circles: Theoretical ratios for the upper mantel models shown in Fig. 4 with the inclusion of a thin top layer (4 km thick) of variable resistivity ρ_s. The lines between open circles and dots indicate the range of possible variability on continents. Model "*d*" and "*d**" show the best agreement with the empirical ratios for continental conditions.

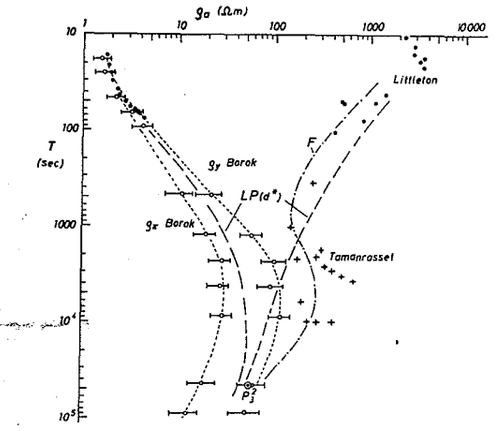

Fig. 6. Magneto-telluric sounding curves $\rho_a(T)$ -T: period-for continental stations with (Borok) and without (Littleton, Tamanrasset) conducting top layer. Dots and crosses according to observations at Borok near Moscow (*Rokityanskiy*, 1962), at Littleton near Boston (*Cantwell*, 1960), and at Tamanrasset in the Sahara (*Launay* et al., 1963); ρ_x and ρ_y refer to north and east polarization of E; the large dot for the diurnal P_3^2-mode has been derived from the diurnal *Z-H* relations at Borok (cf. Appendix). It is in good agreement with the magneto-telluric ρ_a-value for east polarization. The theoretical curves (dashed) have been calculated for the modified *Lahiri and Price* model "*d**" and *Fournier's*(*F*) model in Fig. 4, adding in the case of Borok a top layer with τ=1700 Ω^{-1}. This top layer effects that the ρ_a (T)-curves for model *d** and *F* look alike. The detection of an upper mantle low resistivity layer depends therefore on soundings in areas without surface cover where this layer causes a visible deformation of the $\rho_a(T)$-curve (cf. Fig. 1).

100 km thick. The pertinent formulas can be found, for instance, in *Schmucker* (1970). The source fields are either represented by a single spherical harmonic (D_{st}, *Sq*) or regarded as quasi-uniform for a flat Earth (bays, fluctuations). The resulting inductive scale-length values can be found in Table 1. A top layer of 4 km with ρ_s as uniform resistivity accounts for the variable shielding effect of the outermost shell. We distinguish here between oceans (ρ_s=0.25 Ωm), unfolded sedimentary basins (2 Ωm), standard continental surface layers

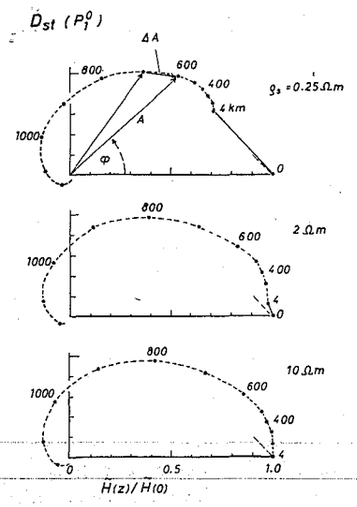

Fig. 7. Attenuation curves in the complex plan for the P_1^0-mode of D_{st}-variations beneath oceans (top), sedimentary basins (center) and standard continents (bottom). Curve parameter is the depth in kilometers and the assumed period is 48 hours (cf. text for details). The vector from the point of origin to any point on the curve gives the amplitude A and the phase lead φ of the tangential magnetic component $\tilde{H}(z)$ at the depth z relative to its surface value $H(0)$. A line element $\Delta A \approx 4\pi\, j/H(0)$ indicates similarly amplitude and phase of the induced current density j, integrated over the pertinent differential increase of z (except for a minor non-inductive portion of the downward attenuation). The main inductive attenuation of D_{st}-variations occurs between 600 km and 1000 km (in mantle depth model d^*). The shielding effect by real oceans is probablly less than indicated by the top curve because the D_{st}-induced current flow along parallels of latitude is broken up by continents.

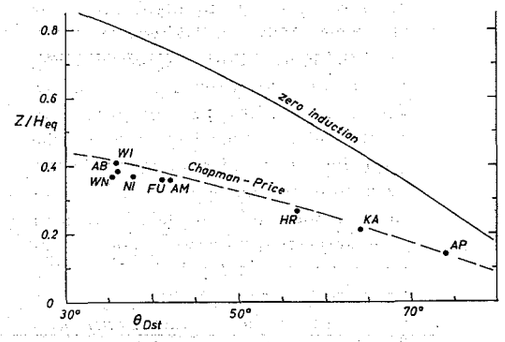

Fig. 8. Z-amplitude of the D_{st}-field as function of geomagnetic co-latitude about 36 hours after the onset of magnetic storms, normalized to the H-amplitude at the equator. It is well below the curve of zero induction (cos ϑ_{Dst}) and it can be explained by a perfectly conducting "core" at 600 km depth (cf. model "e" in Fig. 4). The results from individual observatories are in good agreement with the global mean curve (dashed), thus excluding the possibility of lateral inhomogeneities at that depth (*Grafe*, 1964). AB : Abinger/England, AM : Amberley/New Zealand, AP : Apia/Samoa, FU : Fürstenfeldbruck/Bavaria, HR : Hermanus/South Africa, NI and WN : Niemegk and Wingst/North Germany, WI : Witteveen/The Netherlands.

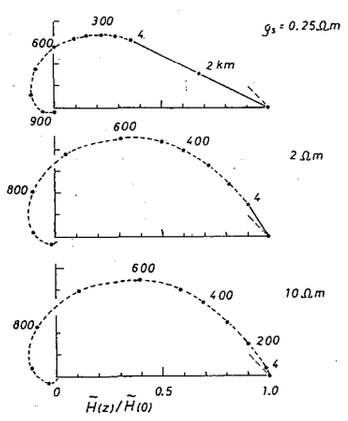

Fig. 9. Attenuation curves in the complex plane for the P_3^2-mode of the 2^{nd} diurnal time harmonic (cf. legend to Fig. 7). Depth range of main induction between 400 and 800 km for continents (center and bottom), but considerable inductive attenuation by large and deep oceans (top) when the continental mantle model d^* used here applies also to the oceanic substructure.

(10 Ωm) and shields (10^4 Ωm).

4. Inferences from D_{st} and Sq-variations

Smoothed storm-time or D_{st}-variations occur when after a magnetic storm the Earth is encircled by an equatorial ring current. During its decay the Earth as a whole is exposed to a uniform field antiparallel to the geomagnetic dipole axis which vanishes exponentially within a few days. Modulations of this ring current field account for ultra-long periodicities in geomagnetic storm-time activity with 27 days and one year as fundamental periods. *Banks* (1969) inferred from their internal part that the steep reduction of resistivity between 400 and 600 km levels off at greater depth, yielding a nearly constant resistivity of 1 Ωm between 1000 and 1500 km.

The ring current source field at a given instant of universal time is well described on the Earth's surface by the spherical harmonic $P_1^0(\cos\vartheta)$ where ϑ denotes the geomagnetic co-latitude (cf. *Appendix*; *Chapman* and *Bartels*, 1940; chap. 20. 11). *Chapman* found that 36 hours after the onset of a magnetic storm the ratio of the internal to external part for the P_1^0-mode is $S_1^0 = 0.35$ with a slight tendency to decreace in time. This is well below the maximum possible ratio of $\frac{1}{2}$ for n=1 and shows that the internal part originates from currents at considerable depth. We infer from Fig. 7 that the main attenuation of D_{st}-variations takes place between 600 and 1000 km.

Chapman's ratio represents a global average, but as it is evident from Fig. 8 regional or local deviations appear to be insignificant (*Grafe*, 1964). Hence, the resistivity distribution beneath 600 km is basically of spherical symmetry.

First indications for lateral non-uniformities come from the study of the diurnal Sq-variations which have their main attenuation in mantle region C of *Bullen's* classification (Fig. 9). In ocean basins we expect an additional strong attenuation in the seawater when we combine a 4 km deep ocean with mantle model "d" or "d^*" (cf. comments to Eq. 18). Induction anomalies of Sq-variations near coastlines and on islands (*Mason*, 1963; *Schmucker*, 1970) support this view, but observations at the seafloor off the Californian coast gave a surprisingly small attenuation by oceanic induction currents, implying that the oceanic substructure is here better conducting than model d^* (*Filloux*, 1967; *Larsen* and *Cox*, 1966; Fig. 12).

The diurnal Sq-variations at a fixed site are quasi-harmonic functions of local time with 24 hours as fundamental period. Their source are two current loops in the day-lit part of the ionosphere, moving for a rotating observer with the Sun around the Earth. This implies that the longitude dependence of the m^{th} time harmonic of Sq is exp (im φ) with φ as longitiude (Eq. 19). In the series of pertinent spherical harmonics of the rank m the first uneven term of the degree $n=m+1$ dominates, in particular during equinoxes (*Chnpman and Bartels*, 1940; chap. 20. 4). Hence, the co-latitude dependence of the m^{th}time harmonic is $P_{m+1}^n(\cos\vartheta_n^m)$ with ϑ_n^m as effective co-latitude for this term (cf. Appendix).

The representation of the Sq-source-field harmonics by a single spherical function can be used as in the case of D_{st}-variations to derive from observations at a single site the

inductive scale-length C_n^m $(m\omega_0)$ and thereby a regional estimate for the ratio S_n^m $(m\omega_0)$ of internal to external part ($\omega_0 = 2\pi$/day). In the absence of local anomalies (s. below) these transfer values reflect the deep resistivity distribution within a lateral range of a few hundred kilometers around the point of observation and they may be compared with those from a global analysis such as *Chapman's*.

This is done in Fig. 10, displaying the C_3^2 and C_4^3 transfers for a number of continental observatories. They have been derived according to Eq. (20) from the diurnal harmonics in Z and the two horizontal components with respect to the local "*Sq*-effective" meridian, inserting for ϑ the "*Sq*-effective" co-latitude ϑ_n^m from Eq. 25 (cf. Appendix). The harmonics have been calculated from the hourly means of twenty quiet days during the years 1932/3 (open circles), 1958 (full circles), and 1965 (triangles), taken from *Price and Wilkins* (1963), *Price and Stone* (1964), and 1965-year books of the observatories.

In the case of the P_3^2-mode we find a fair agreement between the results of *Chapman's* global analysis and those derived from the 2^{nd} *Sq*-harmonic at individual observatories at some distance from the coast. Several stations with a strongly deviating value in the $\rho^* - z^*$ plot are within the range of well known inland induction anomalies. This applies

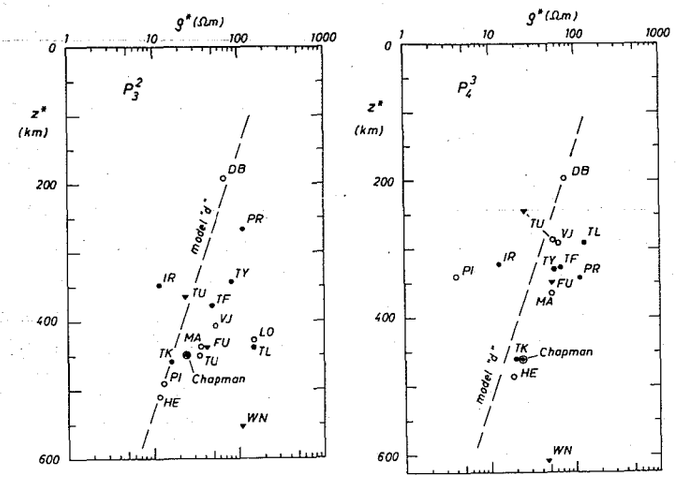

Fig. 10. Modifield apparent reisistivity ρ^* versus depth z^*-plot for the 2^{nd} and 3^{rd} time harmonic of diurnal *Sq*-harmonics, derived from the pertinent Z/H-ratios of individual continental observatories and from *Chapman's* global mean for the ratio of internal to external part (cf. text and Table 1). The cluster of resistivity- depth estimates lies slightly above model "*d*" of *Lahiri and Price*. Their scattering may reflect partially local induction anomalies (WN) and partially regional deviations from the continental norm (TK, HE). DB: DeBilt/The Netherlands, FU: Fürstenfeldbruck /Bavaria, HE: Heluan/Egypt, IR: Irukutsk/Siberia, LO: Lovö /Sweden, MA: Manhay/Belgium, PI: Pilar/Argentina, PR: Pruhonice/Czechoslovakia, TF: Tiflis/Caucasus, TK: Taschkent /Turkmenia. TL: Toledo/Spain, TU: Tucson/Arizona, TY: Tihany/Hungaria, VJ: Val Joyeux/France, WN: Wingst/Germany.

in particular to Wingst in northern Germany (cf. *Untiedt's* contribntion to this volume). It has been shown by *Fanselau* (1968) that the diurnal ranges behave in this area quite anomalously even on a local scale.

Chapman's result for the P_4^3-mode appears not to be representative for the majority of continental stations. The inductive response to the 3^{rd} *Sq*-harmonic yields a clearly reduced scale length z^* of 300 km when compared with the mean z^*-depth of 400 km for the 2^{nd} harmonic. This reduction cannot be explained by the modified model d^* (Table 1) and suggests the presence of even lower resistivities in the uppermost mantle than those given in model d^*. There are notable exemptions from the reduced depth of main attenuation of the P_4^3-mode. The diurnal Z-H relations at the observatories Heluan (Egypt) and Taschkent (USSR) yield for both harmonics large real scale-length values z^* in the order of 500 km, but apparent resistivities ρ^* which are in nearly perfect agreement with model *d*. Here we may have indications for a truly regional deviation from the continental norm, implying that the *Sq*-variations in both areas penetrate with little attenuation deep into an upper mantle of unusually high resistance.

5. Inferences from bay events and fast fluctuations

The spectrum of fast geomagnetic variations is connected to storm-time activity in polar regions. Its prominent feature is the polar electrojet which encircles the polar cap as a current of fluctuating strength and position in about 67° geomagnetic latitude. This jet is partially closed by loops of wide-spread return currents in middle and low latitudes. Bay events are magnetic elementary storms of short duration with $f=1$ cph as representative frequency. A second jet is found above the magnetic dip equator on the day-lit side. Its strength (but *not* its position) fluctuates likewise during polar disturbances.

Both jets provide localized and nearly two-dimensional source fields for geomagnetic induction studies between 1 and 10 cph. Their half-width of a few hundred kilometers is comparable in this frequency range to the skin-depth value of the mantle below 100 km depth. Hence, we may expect some inductive attenuation of the fluctuating jet field in the upper mantle which is detectable at the Earth's surface in form of reduced Z-variations on either side of the jet. The size of geoelectric variations beneath the jet itself is in a similar way an indicator for the depth of penetration when proper regard is given to the limited half-width of the source field. The use of convolution integrals as described in Sect. 1 (Eq. 9) allows a straightforward evaluation of the complicated Z-H and E-H relations in polar and day-time equatorial regions.

First attempts to utilize short-period variations of the polar and equatorial jets for induction studies have been made in the Andes of Peru (*Schmucker* et al., 1967) and on Iceland (*Hermance and Garland*, 1968). The depth of inductive attenuation was found in either case to be surprisingly shallow, suggesting resistivities of only 10 Ωm at about 50 km depth. If these estimates are correct, we have beneath both areas a lens or a channel of highly conducting matter within the uppermost mantle.

At some distance from the jets the variation field of bays and fast fluctuations is

quasiuniform, i.e. the H-amplitude of disturbances is reduced by only a few percent per 100 kilometers toward south. The Z/H-ratio of bays varies in mid-latitudes between 0.3 in regions of maximum depth of penetration into a high-resistance uppermost mantle and less than 0.1 in regions where the inductive attenuation occurs at comparatively shallow depth. This can be due to an intermediate layer of extremely low resistivity or it may reflect a generally reduced resistivity of the upper 200-300 km. The cordillera of western North America and Bavaria are examples for such unusually low Z/H-ratios on a regional scale (cf. Fig. 1 in *Caner*'s and Fig. 8 in *Untiedt's* contribution to this volume).

It is difficult to derive from the mid-latitude Z-H relations of bays and fast fluctuations the normal change of resistivity with depth in any detail because too little is known about the source field geometry. This can be done more effectively with the magneto-telluric E-H relations. The quasi-uniformity of the source field in relation to the depth of penetration justifies the use of the source-field-free *Tikhonov-Cagniard* approximation (Eq. 8). The main difficulty for magneto-telluric soundings between 1 and 10 cph is due to the distoring effect of superficial resistivity gradients, in particular upon E (s. below).

The value of purely geomagnetic deep sounding arises from the sensitivity with which the Z-component of bays reacts in the absence of a significant normal part in mid-latitudes to lateral non-uniformities in ρ. Large Z-amplitudes, yielding a Z/H-ratio of 0.5 and more, are observed only in limited zones, where they depend strongly on the polarization direction of the source field and are therefore anomalous (Sect. 2).

The magneto-telluric impedance E/H, on the other hand, shows almost everywhere a directional dependence in the considered frequency range and thus is anomalous, even where the Z-H relations may be normal. This applies in particular to continental areas at some distance from deep sedimentary basins (cf. Fig. 8 in *Untiedt's* contribution to this volume). Bay events penetrate here with little attenuation through geological formations near the surface and resistivity contrasts within these formations do not produce a sizeable induction anomaly in Z and H. The same applies also to the geoelectric field in the case of E-polarization (Sect. 2). If, however, in the case of H-polarization E is parallel to superficial resistivity gradients, the continuity condition for the electrical current density E/ρ leads to a highly anomalous behaviour in E.

The depth of penetration of bays and fast fluctuation is largely controlled by the electrical properties in the outermost shell, consisting of oceans and continental surface layers above the crystalline basement. This is evident from real scale-length values z^* in Table 1 in dependence of the surface resistivity ρ_s. Large and deep oceans reduce the amplitude of fast variations to such an extent that their induction within the upper mantle becomes insignificant (Fig. 11 and 12).

Because the depth d of oceans is small in comparison to the skin-depth value of seawater at $f=1$ cph, oceans may be treated as parts of an infinitely thin conducting shell of the integrated conductivity $\tau=d/\rho_s$ (Eq. 16). The dimensionless parameter which determines the degree of inductive attenuation in the ocean sheet is

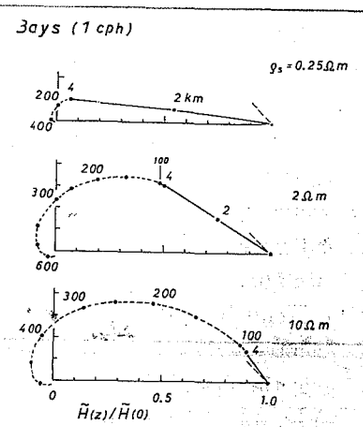

Fig. 11. Attenuation curves in the complex plane for bay events (cf. legend to Fig. 7). They are strongly attenuated by oceans (top). The inductive shielding by continental surface layers above the crystalline basement is large in young sedimentary basins (center), but insignificant elsewhere (bottom). The bulk of deep induction currents flows under normal conditions (model d*) between 150 and 400 km depth.

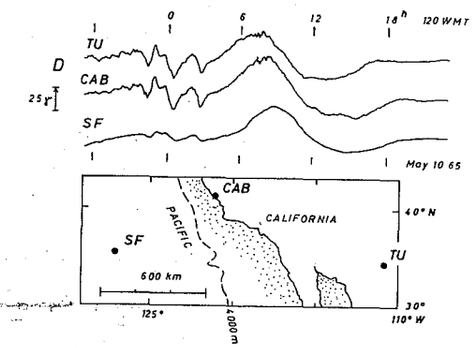

Fig. 12. Variations of the magnetic east component D, recorded simultaneously at the seafloor (SF) off the Californian coast, at the coastal station Cambria (CAB) and at the inland observatory Tucson (TU). The seafloor record when compared with those at CAB and TU shows a distinct lack of high frequencies, reflecting the inductive attenuation by seawater. The amplitude reduction of bays and diurnal variations at the seafloor is however less than to be expected for a continental-type deep resistivity distribution (cf. top curves in Fig. 9 and 11). This implies the presence of very low resistivities at shallow depth (Fig. 13). Adapted from *Filloux* (1967).

$$\eta_s = 4\pi\omega\mu\tau\lambda = (2d\lambda)/p_s^2 \qquad (18)$$

where λ represents either the vertical inductive scale-length $C(\omega, 0)$ for the oceanic substructure, the lateral scale-length of the inducing source field, or the half-width of the ocean, whichever is the smallest length.

The first mentioned vertical scale length accounts for the inductive coupling between oceanic and suboceanic induction currents. It is in the order of 200 km for model d^* (without surface cover) at 1cph (Table 1) and thus the determining one in mid-latitudes. This implies that the assumption of lower mantle resistivities than those in model d^* reduces the relative strength of oceanic induction currents and vice versa.

Observations at the ocean floor off the Californian coast have verified that the expected attenuation of bay events and fast fluctuations exists (Fig. 12). The actual reduction at 1 cph to one quarter of the surface amplitude is slightly less than expected for mantle model d^* (Fig. 11). This discrepancy is even more obvious for the diurnal variations which are hardly attenuated at all at the sea floor (Fig. 9 and 12). Hence, the oceanic mantle appears to be here better conducting than the continental model d^*. This is also indicated by the magneto-telluric impedance E/H at the sea floor from which *Filloux* (1967) inferred a

resistivity of just a few Ω. meters at 25 km depth. It remains to be seen whether this resistivity contrast between the oceanic and continental upper mantle is a world-wide phenomenon.

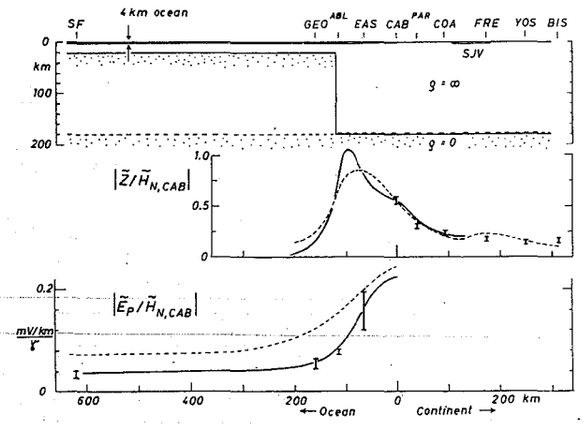

Fig. 13. Cross-section through the coastal anomaly of transient variations in California at f=1cph. The profiles extend in north-easterly direction from a seafloor station SF to Bishop (BIS), 250 km inland from the coastal station Cambria (CAB, cf. Fig. 12). The Z-and E-variations parallel to the coast (E_p) have been normalized with the horizontal variations perpendicular to the coast (H_N) at Cambria. The simple ocean-edge model (dashed) with a perfectly conducting mantle at the uniform depth of 180 km explains correctly the observed inland anomaly in Z (center), but not the oceanic E_p (bottom). This discrepancy can be removed by assuming a step-wise reduction of the depth of the perfect conductor to 20 km near the continental margin (solid curves). Notice that this additional change in the deep resistivity structure has only a secondary effect upon the anomalous behaviour in Z. Adapted from *Filloux* (1967) and *Schmucker* (1970). SJV: SanJoaquin valley (sedimentary basin),

In spite of these complications the coastal anomaly of bay events along the Californian coast is basically an edge-effect of the ocean itself because the known induction currents in the seawater are sufficiently strong to explain in this way the observed anomaly on land (Fig. 13). The same will apply to other coastal anomalies (cf. *Parkinson*, 1962) and it shows that a representative resistivity model for the oceanic substructure depends on observations at sea.

The inductive attenuation of bays beneath continents occurs predominantely between 100 and 300 km depth, when the resistivity of the geological formations is in the order of 10 Ωm or higher. This gives an integrated conductivty of $\tau \leqq 400\ \Omega^{-1}$ for d=4 km (Fig. 11, bottom curve). Therefore it was originally thought that induction anomalies at some distance from coastlines involve deep induction currents from the cited depth range. This view had to be revised when magneto-telluric observations revealed that deep sedimentary basins have integrated conductivities of 2000 Ω^{-1} and more, yielding $\eta_s \approx 1$ as inductive parameter for 1 cph and λ=200 km (*Porstendorfer*, 1965; *Fournier*, 1966).

Hence, we have to expect even on continents superficial induction currents of considerable strength which are bound to sedimentary basins and reduce here effectively the induction in the underlying mantle (Fig. 11, central curve). The interpretation of inland induction anomalies is therefore complicated by the existence of a superficial and deep system of induction currents, separated by the highly resistive crust and uppermost mantle but coupled electromagnetically by mutual induction.

A local concentration of near-surface currents appears to be the cause of those induction anomalies which are common to the boundaries of sedimentary basins and similar geological structures of high integrated conductivity.

The size and spatial half-width of these *surface anomalies* depend to some extent (i) on the depth to the good conductor in the Earth's mantle (which can be studied in this way) and (ii) on the connection which such structures have among themselves and to open oceans. For instance, induction currents from the Atlantic ocean find a free access to the North German basin and this may explain the unusually large edge anomaly along the borders of this basin (cf. *Untiedt's* contribution). The San Joaquin valley, an embayment of comparable integrated conductivity in California, is cut off from the Pacific by a mountain barrier and thus produces only a second-order induction anomaly (*Schmucker*, 1970).

A second class of induction anomalies of bay events can arise from non-uniformities in the upper mantle above 200 km depth, providing that the resistivity changes here laterally by at least an order of magnitude on local scale. A likely source for such *deep anomalies* are lenses or channels of low resistivity ($\varrho \approx 10\ \Omega$m) within the uppermost 100 km. As shown in Fig. 13 deep-seated resistivity anomalies can be largely obscured by superficial resistivity contrasts in the same region. Hence, their unambiguous identification requires that the strength and distribution of superficial induction currents is known quite accurately. This is usually not the case and at the present state only a few of the reported induction anomalies of bays can be classified with some confidence as deep anomalies (Mould Bay, eastern boundary of the Rocky Mountains, Andes, Hungary, Lake Baikal; cf. the respective contributions to this volume, also *Vanjan and Kharin*, 1967).

Here progress can de made (i) with more elaborate model calculations for the surface effect, (ii) with scale-model experiments (*Parkinson*, 1964; *Rankin* et al., 1965; *Dosso*, 1966; *Grenet and Loeb*, 1969), and (iii) with measurements of the superfical current density in situ. Such measurements can be made in two ways. In regions where the integrated conductivity of the geological formations above the crystalline basement can be reliably estimated it is sufficient to observe the tangential electrical field E at the surface. For slow variations (cf. comment to Eq. 16) we may treat E as a constant within these formations and set $j=\tau E$ with j as integrated current density per unit length. Observations of the attenuated horizontal variations H^- below the surface layers, for instance in deep bore holes, yield in $4\pi \boldsymbol{j} = \boldsymbol{n} \times (\boldsymbol{H}^+ - \boldsymbol{H}^-)$ directly the integrated current density between the depth of observation and the surface; $\boldsymbol{n}$ is a unit vector pointing upwards and $\boldsymbol{H}^+$ denotes the horizontal component of the transient magnetic vector at the surface.

The magnetic field of a thus determined system of superficial currents can be found with the formula of *Biot-Savart*. It yields when subtracted from any observed induction anomaly that portion which is due to anomalous deep induction currents in the mantle. These currents may be partially coupled to those at the surface by mutual induction in a stratified "normal" substructure and only after the removal of this secondary effect is the "surface correction" complete. Any remaining part of the induction anomaly is then

to be regarded as being of truly deep origin.

Appendix: Source field presentation by a single spherical harmonic (to Sect. 4)

In the analysis of slow and therefore deeply penetrating variations it is necessary to take the sphericity of the Earth into account. Let (r, ϑ, φ) denote spherical coordinates. Each frequency harmonic of the source field as function of co-latitude ϑ and longitude φ on the Earth's surface $r=a$ is expanded into a series of spherical surface harmonics of the degree n and order m, e.g.

$$\bar{Z}(\omega, \vartheta, \varphi)=\sum_{n=1}^{\infty}\sum_{m=0}^{n} Z_m{}^n(\omega)P_m{}^n(\cos\vartheta)e^{im\varphi}. \qquad (19)$$

The inductive response of an Earth of spherical symmetry is expressed by a series of transfer values $C_n{}^m(\omega)$ which as inductive scale-length contain the information about the internal resistivity distribution $\rho(r)$.

Let H_ϑ rnd H_φ, respectively E_ϑ and E_φ, denote the tangential components of the transient magnetic and electric field vector in ϑ and φ direction. The ratio Z/H ratio of vertical to tangential magnetic variations for a single spherical mode is a function of co-latitude and different for the two orthogonal tangential directions on the Earth's surface, viz.

$$Z_n{}^m(\omega)=ik_nC_n{}^m(\omega)\begin{cases}\dfrac{inP_n{}^m}{dP_n{}^m/d\vartheta}\cdot H^n{}_{\vartheta,n}(\omega)\\[2ex] \dfrac{n\sin\vartheta}{m}\cdot H^m{}_{\varphi,n}(\omega)\end{cases} \qquad (20)$$

where $k_n=(n+1)/a$ is an equivalent to the wave number k in *Eq.* 4 (a: Earth's radius). The impedance ratio E/H of tangential geo-electric to magnetic varations for a single spherical mode is in contrast independent of ϑ and equal for the two orthogonal directions, viz.

$$\left.\begin{matrix}-E^m{}_{\vartheta,n}(\omega)/H^m{}_{\varphi,n}(\omega)\\ E^m{}_{\varphi,n}(\omega)/H^m{}_{\vartheta,n}(\omega)\end{matrix}\right\}=i\omega\mu C_n{}^m(\omega) \qquad (21)$$

in correspondence to Eq. 4.

Eq. 20 implies that the harmonics of H_ϑ and H_φ are out-of-phase, obeying the relation

$$\sin\vartheta\frac{dP_n{}^m}{d\vartheta}H^m{}_{\varphi,n}=imP_n{}^m\,H_{\vartheta,n}{}^m. \qquad (22)$$

The ratio of internal to external parts of the magnetic surface field follows from

$$S_n{}^m(\omega)=\frac{1-k_nC_n{}^m(\omega)}{\dfrac{n+1}{n}+k_nC_n{}^m(\omega)} \qquad (23)$$

(cf. Eq. 6). If the downward attenuation is determined solely by the source field geometry ($S_n{}^m=0$) we have $C_n{}^m=1/k_n$. If, to the contrary, the downward attenuation is purely inductive, so that $k_n|C_n{}^m|\ll 1$, $S_n{}^m$ approaches $n/(n+1)$ as upper limit and $C_m{}^n(\omega)\approx C(\omega, 0)$ becomes independent of the order and degree of the source field harmonic. It can be converted as function of frequency into an apparent resistivity $\rho_a(\omega)$ according the to *Tikhonov-Cagniard* definition or as function of depth z^* into a modified apparent resistivity ρ^* by setting as in *Eq.* 7

$$C_n{}^m(\omega)=z^*(\omega)-\frac{i}{2}p^*(\omega) \qquad (24)$$

for all values of n and m; $\rho^*=2\pi\omega(p^*)^2$ is the resistivity of a uniform substitute conductor of the radius $a-\left(z^*-\frac{1}{2}p^*\right)$ at the considered frequency ω, provided that the argument of $C_n{}^m$ lies between-45° and-90°.

The representation of global source fields by a single spherical harmonic has to be in agreement with Eq. 22. This implies in the case of the zonal D_{st}-field (m=0) that the tangential magnetic component H_φ normal to the "D_{st}-effective" meridian (which is more or less the geomagnetic meridian) is zero. A corresponding "*Sq*-effective" meridian is found from the condition that the diurnal time harmonics of H_ϑ and H_φ when referred to it have a phase difference of 90°. The "*Sq*-effective" co-latitude $\vartheta_n{}^m$ of the point of observation for the mth time harmonic follows from the ratio $H^m{}_{\vartheta,n}/H^m{}_{\varphi,n}=\alpha_n{}^m\cdot i$ where $\alpha_n{}^m$ is a real number and $n+m=1$. Observing that $P_{m+1}{}^m(\cos\vartheta)\sim\sin^m\vartheta\cos\vartheta$ we obtain from Eq. 22

$$\alpha_n{}^m=tg\vartheta_n{}^m\sin\vartheta_n{}^m.\ m^{-1}-\cos\vartheta_n{}^m \qquad (25)$$

as implicit equation for the determination of $\vartheta_n{}^m$.

Monographs and Review Articles

Berdichevskiy, M.N., (*Electrical sounding with the method of magneto-telluric profiling*), Nedra Press, Moscow, 1965.

Chapman, S., and J. Bartels, *Geomagnetism*, Clarendon Press, Oxford, 1940.

Fournier, H.G., Essai d'un historique des connaissances magneto-telluriques, Note Institut de Physique du Globe No. 17, Fac. Science-Univ. Paris, 1966. (Bibliography)

Keller, G.V., and F.C. Frischknecht, *Electrical methods in geophysical prospecting*, Pergamon Press, Oxford, 1966.

Madden, T.R., and C.M. Swift, Magneto-telluric studies of the electrical conductivity structure of the crust and upper mantle, in *The Earth's crust and upper mantle*, edited by V.V. Beloussov and J.Hart, Geophys. monograph No. 13 of the Am. Geophys. Union, Washington D.C., 1969.

Price, A.T., Magnetic variations and telluric currents, in *The Earth's mantle*, edited by T.F. Gaskell, Academic Press, London, 1967.

Price, A.T., Electromagnetic induction within the Earth, in *Physics of geomagnetic phenomena*, edited by S. Matsushita and W.H. Campbell, Academic Press, New York, 1967.

Rikitake, T., *Electromagnetism and the Earth's interior*, Elsevier, Amsterdam, 1966.

Wait, J.R., *Electromagnetic waves in stratified media*, Pergamon Press, Oxford, 1962.

Wiese, H, *Geomagnetische Tiefentellurik*. Deutsche Akad. Wiss. Berlin-Geomagn. Institut Potsdam, Abh. No. 36, 1965.

References

Banks, R.J., Geomagnetic variations and the electrical conductivity of the upper mantle, *Geophys. J.*, **17**, 457-487, 1969.

Cagniard, L., Basic theory of the magneto-telluric method of geophysical prospecting. *Geophysics*, 18,

605–635, 1953.

Cantwell, T., Detection and analysis of low frequency magneto- telluric signals, *Ph. D. Thesis, Dept. Geology and Geophysics, M.I.T.*, 1960.

Dosso, H.W., Analogue model measurements for electromagnetic variations near vertical faults and dykes. *Canada. J. Earth Sc.*, **3**, 287-303, 1966.

Everett, J.E., and R.D. Hyndman, Geomagnetic variations and electrical conductivity structure in southwestern Australia, *Phys. Earth Planet. Interiors*, **1**, 24–34, 1967.

Fanselau, G., The use of range-differences for the interpretation of conductivity anomalies, *Phys. Earth Planet. Interiors*, **1**, 177-180, 1968.

Fanselau, G., and R. Treumann, Zur geomagnetischen Tiefensondierung, *Pure and Appl. Geophys.*, **65**, 54–72, 1966.

Filloux, J.H., Oceanic electric currents, geomagnetic variations and the deep electrical conductivity structure of the ocean-continent transition of central California, *Ph.D. Thesis. Univ. of California, San Diego*, 1967.

Fournier, H.G., S.H. Ward, and H.F. Morrison, Magneto-telluric evidence for the low velocity layer, Space Sc. Lab. Univ. of California, Berkeley, Techn. Rep. No. 4, 1963.

Grafe, A., Die Bedeutung der Abweichungen geomagnetischer Tagesmittel vom sogenannten Normalwert für die Analyse des geomagnetischen Ringstromeffektes. Deutsche Akad. Wiss. Berlin-Geomagn. Institut Potsdam, *Abh. No.* 31, 1964.

Grenet, G., and J. Loeb, Représentation simplifée d'un système de conducteurs explorés en magnétotellurique, *C.R.Acad. Sc. Paris*, **268**, Ser.B, 1045–1048, 1969.

Hasegawa, M., Representation of the field of diurnal variations by the method of graphical integration,, *Proc. Imp. Acad. Tokyo*, **12**, 225-228, 1936.

Hermance, J.F., and G.D. Garland, Deep electrical structure under Iceland, *J. Geophys. Res.*, **73**, 3797–3800, 1968.

Hughes, H., The pressure effect on the electrical conductivity of Peridotit, *J. Geophys. Res.*, **60**, 187–191, 1955.

Lahiri, B. N., and A.T. Price, Electromagnetic induction in non-uniform conductors, and the determination of the conductivity of the Earth from terrestrial magnetic variations, *Phil. Trans. Roy. Soc. London Ser. A*, **237**, 509–540, 1939.

Larsen, J., and C. Cox, Lunar and solar daily variation in the magneto-telluric field beneath the ocean, *J. Geophys. Res.*, **71**, 4441–4445, 1966.

Launay, L., Touitou J., and G. Grenet, La conductibilité électrique du manteau supérieur, *Ann. Geophys.*, **19**, 180–183, 1963.

Mason, R.G., Spatial dependence of time variations of the geomagnetic field in the range 24hrs–3mins on Christmas Island, *Geophys. Dept. Imperial College London, Ref.* 63–3, 1963.

Parkinson, W.D., Direction of rapid geomagnetic fluctuations, *Geophys. J.*, **2**, 1–14, 1959.

Parkinson, W. D., The influence of continents and oceans on geomagnetic variations, *Geophys.J.*, **6**, 441–449, 1962.

Parkinson, W.D., Conductivity anomalies in Australia and the ocean effect, *J. Geomag. Geoelect.*, **15**, 222–226, 1964.

Porstendorfer, G., Methodische und apparative Entwicklung magneto-tellurischer Verfahren mit Anwendung auf die Tiefenerkundung im Bereich der norddeutschen Leitfähigkeitsanomalie, Deutsche Akad. Wiss. Berlin-*Institut f. Geodynamik Jena, Heft* 3, 1965.

Price, A.T., The induction of electric currents in non-uniform thin sheets and shells, *Quart. J. Mech. and Applied Math.*, **2**, 283–310, 1949.

Price, A.T., and G.A. Wilkins, New method for the analysis of geomagnetic fields and their application to the *Sq* field of 1932–3, *Phil. Trans. Roy. Soc. London Ser. A*, **256**, 31–98, 1963.

Price, A.T., and D.J. Stone, The quiet-day magnetic variations during the IGY, Annals of the International Geophysical Year, **35**, 64–269, *Pergamon Press, Oxford*, 1964.

Rankin, D., G.D. Garland, and K. Vozoff, An analog model for the magnetotelluric effect, *J. Geophys. Res.*, **70**, 1939–1945, 1965.

Rikitake, T., Electromagnetic induction within the Earth and its relation to the electrical state of the Earth's interior. *Bull.Earthqu. Res. Inst. Tokyo Univ.*, **28**, 45–100, 219–283, 1950.

Rikitake, T., Possibility of detecting the mantle low-velocity layer by geomagnetic deep sounding, *Bull. Earthqu. Res. Inst. Tokyo Univ.*, **40**, 495–509, 1962.

Rikitake, T., Electromagnetic induction within non-uniform plane and spherical sheets, *Bull. Earthqu. Res. Inst. Tokyo Univ.*, **45**, 1229–1294, 1967.

Rikitake, T., Electromagnetic induction in uniform and non-uniform sheets underlain by an undulating perfect conductor, *Earthqu. Res. Inst. Tokyo Univ.*, **46**, 361–384, 1968.

Rokityanskiy, I.I., (Magneto-telluric sounding curve for the observatory Borok), *Izv. AN SSSR seriya geofiz. No.* 4, 679–680, 1962.

Scheube, H.G., An evaluation method for geomagnetic deep sounding, its derivation and practical use, *Geophys. Prospecting*, **14**, 149–167, 1966.

Schmucker, U., Erdmagnetische Tiefensondierung in Deutschland 1957/59: Magnetogramme und erste Auswertung, Akad. Wiss. Goettingen, Math.-Phys. Kl. *Beitraege z. Internat. Geophys. Jahr, Heft* **5**, 1959.

Schmucker. U., S.E. Forbush, O. Hartmann, A.A. Giesecke, M. Casaverde, J. Castillo, R. Salgueiro, S. del Pozo, Electrical conductivity anomaly under the Andes, Yearbook **65**, 11–28, *Carnegie Institution of Washington, Washington D.C.*, 1967.

Schmucker, U., Anomalies of geomagnetic variations in the southwestern United States, Bulletin Scripps Institution of Oceanography, **13**, *Univ.of California Press*, 1970.

Tikhonov, A.N., and N.V. Lipskaya, (Terrestrial electric field variations), *Doklady Akad. Nauk SSR*, **87**, 547–550, 1952.

Vanjan, L.L., and E.P. Kharin, (Magnetic depth sounding in the lake Baikal area), in Regional geophysical investigations in Siberia, Acad. *Sc. USSR, Siberian dept.*, 1967.

Wait, J.R., Propagation of radio waves over a stratified ground. *Geophsics*, **18**, 416–422, 1953.

Wiese, H., Geomagnetische Tiefetellurik Teil II: Die Streichrichtung der Untergrundstrukturen des elektrischen Widerstandes, erschlossen aus geomagnetischen Variationen, *Geofisica pura i appl.*, **52**, 83–103, 1962.

Wright, J.A., The magnetotelluric and geomagnetic response of two-dimensional structures, Institut f. Geophys. und Meter. *Techn. Univ. Braunschweig, Gamma* **7**, 1969.